Current Trends in Biotechnology and Pharmacy
Vol. 19(3) 2444-2461, July 2025, ISSN 0973-8916 (Print), 2230-7303 (Online)
DOI: 10.5530/ctbp.2025.3.29



# Computational Study on Marine Algae-Derived Octaphlorethol A as a Potential Inhibitor of Beta-Secretase for Alzheimer's Therapy

**Bhukya Venkatesh[1], Moni Philip Jacob Kizhakedathil[2], HemaNandini Rajendran Krishnamoorthy[3], Ramanathan Karuppasamy[3,*], Sudarshana Deepa Vijaykumar[4,*]**

[1]Department of Hydro and Renewable Energy, Indian Institute of Technology Roorkee, Uttarakhand, India – 247667.
[2]Department of Chemical and Biological Engineering, Monash University, Clayton, VIC, Australia - 3800
[3]Department of Biotechnology, School of Bio Sciences and Technology, Vellore Institute of Technology, Vellore, Tamil Nadu, India – 632014.
[4]Department of Biotechnology National Institute of Technology, Tadepalligudem Andhra Pradesh-534101, India

***Corresponding Author**: sudarshanadeepa@nitandhra.ac.in

## Abstract

Alzheimer's disease is a progressive neurodegenerative disease that mainly affects people above the age of 65 years. Current treatments focus to reduce the symptoms of the disease but do not target the cause. In the current study, we targeted on the β-secretase belonging to the amyloidogenic pathway. Secondary metabolites from marine organism are often unexplored. In the current study, we explored about 202 such metabolites to check their potential to inhibit β-secretase. A library of secondary metabolite structures was downloaded from the PubChem database. The three-dimensional protein structures - β-secretase (PDB ID: 1M4H) was downloaded from PDB database. The ligands and the proteins were subjected to energy minimization using UCSF Chimera software employing an AMBER force field. Molecular docking was performed to evaluate the binding affinity of ligands against the β-secretase using AutoDock Vina. Semagacestat was used as standard. Post dock analysis was performed using Ligplot plus and PLIP server. ADMET analysis was performed using SWISS ADME and PROTOX II servers. Among the 202 compounds, Octaphlorethol-A showed higher binding affinity towards the enzymes β-secretase when compared to standard. In addition, molecular dynamic simulation studies confirmed that the compounds form relatively stable complex than the standard drug. Moreover, the ADMET analysis indicates that octaphlorethol-A could be chosen as a potential drug candidate. In the future, these compounds could be used as potential leads and evaluated via in-vitro and in-vivo experimental studies to validate the results.

**Keywords:** Alzheimer's disease, β-secretase, Molecular docking, Octaphlorethol-A, ADME, Toxicity

## Introduction

Alzheimer's disease (AD) is a neurological disorder marked by the buildup of abnormal proteins in the brain, including beta-amyloid and tau, which results in neuronal loss and cognitive decline (1). AD primarily affects people over 65 and is among the most common forms of dementia. Alzheimer's disease (AD) is expected to increase in the coming years, leading to an

Current Trends in Biotechnology and Pharmacy
Vol. 19(3) 2444-2461, July 2025, ISSN 0973-8916 (Print), 2230-7303 (Online)
DOI: 10.5530/ctbp.2025.3.29


estimate 152 million cases globally by 2050 (2). The most common symptoms of AD include memory loss, difficulty completing familiar tasks, poor judgment and decision-making abilities, mood swings, personality changes, confusion about time and place, trouble with spatial orientation, difficulty with language and communication, misplacing items, and losing the ability to retrace steps. The risk of developing AD extends with age, with most cases affecting people above the age 65. Nevertheless, early onset Alzheimers can also affect people as young as their 30's and 40's (3). The brains of patients diagnosed with AD were characterized by chronic inflammation, plaques, and tangles, which eventually lead to neuronal cell death (4-5). Many theories are being presented to explain the causes of AD, including vascular dysfunction hypothesis, cholinergic, lymphatic system, inflammation, and metal ion hypothesis. Theories like the amyloid cascade, mitochondrial cascade, calcium homeostasis, and tau propagation hypothesis focus on pathological events after the occurrence of AD (6). There is currently no therapy for the treatment of Alzheimer's disease. Treatments for AD mainly focus on the management of AD-associated symptoms. Acetylcholine esterase inhibitors are presently employed to enhance cholinergic neurotransmission and reduce the hydrolysis of Acetylcholine in the brain. Even though these medications are quite effective, they are also associated with several side effects (4-5).

The amyloid cascade, also known as the amyloid or Aβ hypothesis, posits the formation and pathogenesis of beta-amyloid plaques and their role in Alzheimer's disease (AD). Amyloid precursor proteins (APP) are necessary for neuronal development and repair. APP, a transmembrane protein, has two mechanisms for the cleavage of transmembrane protein APP: the non-amyloidogenic pathway, which involves α-secretase, and the amyloidogenic pathway, which involves β-secretase. In the amyloidogenic pathway, β-secretase breaks down APP to form the soluble fragment (sAPP-β). γ-secretase cleaves APP's C-terminal fragment 99 (APP-CTF99 or βCTF), resulting in the production of amyloid β peptides, Aβ-40 and Aβ-42, and the amyloid intracellular domain (AICD) (6) (Fig. 1).

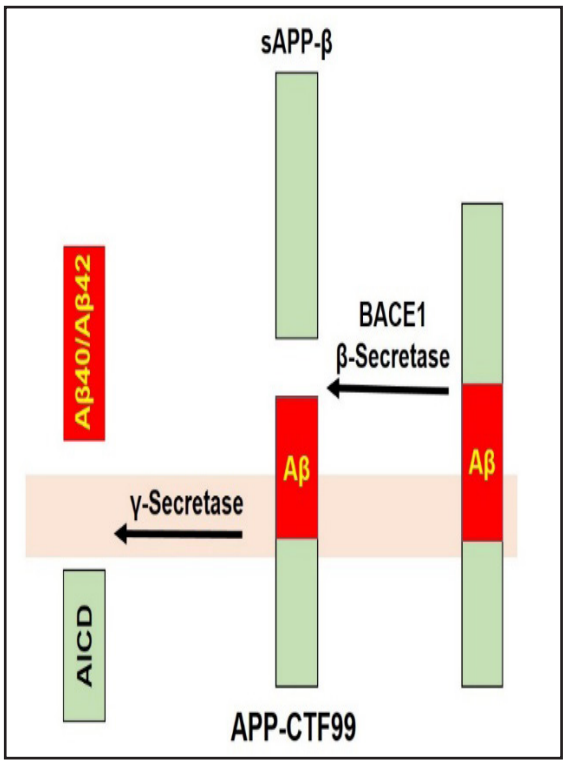


Figure 1: Amyloidogenic Pathway of Alzheimer's Disease: Processing of APP Protein by β-Secretase and γ-Secretase Leading to Amyloid Beta Plaque Accumulation in Neurons

In healthy individuals, APP is divided by β-secretase and then by γ-secretase, resulting in soluble amyloid-β fibers (Aβ), which are then degraded and recycled outside the cell. In AD patients, the ability to degrade these proteins is diminished, leading to the accumulation of amyloid plaques. Aβ sticky proteins join to form insoluble β amyloid plaque in the neural cell and create tangles. The formation of such plaques hinders the relay of neuronal signals and blocks the brain's blood vessels, leading to bleeding, amyloid angiopathy, and the rupture

of cells (4, 8). This study focuses on the amyloidogenic pathway and proposes to examine compounds that could potentially inhibit the activity of β and γ-secretase, thereby reducing the formation and accumulation of Aβ plaques.

Humans continue to strive to find new drugs to treat Alzheimer's disease (AD). Current therapies for AD, including non-disease modifying treatments and symptom relief medications such as Donepezil, Avagacestat, Semagacestat, Rivastigmine, and Galantamine, have limited effectiveness and often fail in clinical trials (9). As a result, the search for new AD treatments remains urgent. Research on marine organisms has gained traction since the early 21st century, though the potential of these organisms remains underexplored (10). Marine organisms produce novel and unique metabolites, likely due to high environmental conditions due to high pressure, temperature, and salinity. These secondary metabolites include a wide range of compounds, such as vitamins, enzymes, herbicides, antibiotics, anti-tumor agents, anti-parasitics, and antivirals (10 – 12). In the present study, we analyzed approximately 200 metabolites from various marine organisms. These compounds were docked with β-secretase to explore their binding potential. Additionally, analyses of ADMET (absorption, distribution, metabolism, excretion, and toxicity) are conducted based on the potential compound.

## Materials and Methods

### *Literature Research*

This study aims to identify secondary metabolites from marine organisms and assess their potential to inhibit the β-secretase enzyme. A literature review was conducted using PubMed and Scopus with keywords such as "Secondary metabolites," "GC-MS analysis," "Marine-derived," and "Bioactive compounds." Approximately 200 compounds from marine algae, bacteria, seaweed, and sponges were selected to evaluate their therapeutic properties (13-15).

### *Ligand preparation*

The PubChem database (https://pubchem.ncbi.nlm.nih.gov/) was utilized to retrieve the two and three-dimensional structure of the ligands. The two-dimensional structures were converted to three-dimensional structures. The ligand files were then energy minimized via UCSF Chimera with the AMBER force field (16). These energy-minimized ligands were subsequently used for further docking. Semagacestat was used as the standard in this study.

### *Protein target and preparation*

For this study, the β-secretase protein from the Secretase pathway, involved in generating beta-amyloid peptides, was selected. So, the Crystal Structure of Beta-secretase (PDB ID: 1M4H) was obtained via the RSCB PDB database (https://www.rcsb.org/) (17). Before docking, bound organic, solvent, and inorganic molecules were removed using PyMol software (18). The protein underwent energy minimization using UCSF Chimera with the AMBER force field.

### *Molecular docking*

AutoDock Vina was used to dock the ligands to the targeted proteins (19). Active site docking was performed using literature data to determine the active site residues of the proteins. The grid box parameters for β-secretase were established as follows: size in x, y, and z dimensions were 60, 50, and 40, respectively, with centre grid coordinates of 22.347, 33.883, and 24.855, respectively. The docking runs were carried out in triplicate, and the outcomes are reported as Mean ± Standard variation. Simultaneously, the free energy values in kcal/mol were calculated for every docked compound toward the targeted proteins (20). Moreover, the bind site locations and fundamental molecular interactions were investigated using the Protein-Ligand Interaction Profiler (PLIP) and Ligplot Plus v2.2 (21-22).

### *Molecular dynamics and simulation analysis*

The dynamic characteristics of targeted molecules within their biomolecular structures were investigated using GROMACS software version 2020.2. The protein's structural framework was initially established by employing the CHARMM36 force field. Subsequently, the protein-ligand complexes were immersed in a dodecahedral box utilizing the SPC (single point charge) water-based model for solvation. Energy minimizations were conducted using the steep descent algorithm to optimize the complexes. Further, the SHAKE algorithm was utilized to maintain fixed hydrogen binding lengths. Accurate electro-static interaction and bond length computations were enforced via the particle mesh Ewald (PME) method and the LINCS algorithm, respectively. Moreover, the system structure was equilibrated under NVT (canonical ensemble) and NPT (isothermal-isobaric ensemble) conditions at 300 K and 1 bar for 100 picoseconds. Subsequently, a production simulation of 100 nanoseconds with a 2-femtosecond integration time step was performed for the protein-ligand system. Utilizing GROMACS tools, key parameters such as Root Mean Square Deviation (RMSD), Root Mean Square Fluctuations (RMSF), hydrogen bonding patterns, Solvent Accessible Surface Area (SASA), and Radius of Gyration were assessed the structural stability of the protein-ligand complex.

### *ADMET Analysis*

Molecular descriptors and (ADME) Absorption, Distribution, Metabolism, and Excretion properties with ligands were evaluated utilizing the SwissADME tool (http://www.swissadme.ch/) (23), while the toxicological profiles were anticipated employing Protox II online server (24). Assessment of their ADMET properties enables the characterization of promising compounds, enabling the identification of potential lead and ligand with significant disqualifies their drawbacks.

## Results and Discussion

### *Molecular docking*

De novo discovering drugs is a lengthy, expensive, and multistage process. Nowadays, computer-aided drug discovery is gaining popularity owing to its precision and is used hand in hand with in vitro assays. This dramatically reduces the time and cost involved in drug discovery. Even though the results may not be figuratively conclusive, they may serve as the foundation for future in-vivo and vitro studies and further strengthen their result. Molecular docking is a commonly used computer-aided drug discovery method. Docking visualizes the orientation of small molecules attached to targeted proteins. Docking involves several scoring algorithms that calculate their ligand binding energy with this protein. The most stable complex was formed with the lowest binding energy between the protein-ligand complex (25 – 26).

Docking investigations involving 202 compounds, specifically secondary metabolites sourced from marine organisms, were conducted employing AutoDock Vina. The three-dimensional structure of these compounds was utilized from the PubChem database, and before docking analysis, ligands underwent energy minimization using UCSF Chimera with an AMBER force field. Semagacestat served as the reference standard throughout this study. Protein structures were obtained as PDB files from the PDB database and subjects towards cleaning and energy minimization before docking. All simulations were performed in triplicate. Mean binding energies and standard deviations, sourced accordingly, are presented in Table 1. Post towards docking scrutiny of their protein ligand complex was executed utilizing PLIP and Ligplot Plus, focusing on binding interactions encompassing hydrophobic interactions, hydrogen bond and π-cation interactions, as detailed in Table 2.

Table 1: Docking scores (in kcal/mol) for compounds derived from various marine organisms against β-secretase were determined. The experiments were conducted in triplicate, and the results are reported as the mean ± standard deviation.

| S.No. | Compounds | Binding Energy (kcal/mol) |
|---|---|---|
| 1 | Fucoxanthin | -6.87 ± 0.12 |
| 2 | Fucosterol | -7.6 ± 0.17 |
| 3 | Dieckol | -9.07 ± 0.12 |
| 4 | eckol | -7.37 ± 0.12 |
| 5 | 7-phloroeckol | -7.87 ± 0.12 |
| 6 | phlorofucofuroeckol A | -7.97 ± 0.12 |
| 7 | dioxinodehydroeckol | -8.97 ± 0.12 |
| 8 | Phlorofucofuroeckol B | -8.73 ± 0.06 |
| 9 | 8,8'-bieckol | -8.87 ± 0.12 |
| 10 | 6,6'-bieckol | -8.37 ± 0.12 |
| 11 | Fucoidan | -5.67 ± 0.12 |
| 12 | κ-carrageenan | -7.37 ± 0.12 |
| 13 | Oleic acid | -5.77 ± 0.12 |
| 14 | Methyclothiazide | -6.27 ± 0.12 |
| 15 | Sargachromenol | -7.67 ± 0.12 |
| 16 | Glycidyl palmitate | -4.17 ± 0.12 |
| 17 | 2-(alpha-D-galactosyl)glycerol | -5.67 ± 0.12 |
| 18 | Caulerpin | -7.67 ± 0.12 |
| 19 | 24-hydroperoxy | -7.07 ± 0.12 |
| 20 | 24-vinylcholesterol | -7.87 ± 0.12 |
| 21 | α-Bisabolol | -6.77 ± 0.12 |
| 22 | (5E,10Z)-6,10,14-trimethylpentadeca | -5.37 ± 0.12 |
| 23 | Saringosterol | -8.17 ± 0.12 |
| 24 | Glycidyl oleate | -4.97 ± 0.12 |
| 25 | Pheophytin A | -6.4 ± 0 |
| 26 | Dimethylsulfoniopropionate | -3.77 ± 0.12 |
| 27 | Zonarol | -6.67 ± 0.12 |
| 28 | dioxinodehydroeckol | -9.07 ± 0.12 |
| 29 | Phorbol-13-acetate | -5.27 ± 0.12 |
| 30 | Tramiprosate | -4.47 ± 0.12 |
| 31 | Laminarin | -9.17 ± 0.12 |
| 32 | Tramiprosate | -4.47 ± 0.12 |

| | | |
|---|---|---|
| 33 | Eut-Guaiane sesquiterpene | -6.67 ± 0.12 |
| 34 | p-Menth-1-en-3-ol | -5.27 ± 0.12 |
| 35 | 2-dichloro-5-[(E)-2-chloroethenyl]-1,5-dimeth-ylcyclohexane | -4.87 ± 0.12 |
| 36 | triphloroethol A | -6.77 ± 0.12 |
| 37 | Dioxinodehydroeckol | -9.07 ± 0.12 |
| 38 | N-ethanolic monapilosine | -6.47 ± 0.12 |
| 39 | Diisooctyl phthalate | -4.47 ± 0.12 |
| 40 | nonaenoic acid | -6.17 ± 0.12 |
| 41 | Glucobrassicin | -7.33 ± 0.06 |
| 42 | 3-Deoxy-D-Lyxo-Heptopyran-2-ularic Acid | -6.53 ± 0.06 |
| 43 | Eicosapentaenoic acid | -5.27 ± 0.12 |
| 44 | Pentabromopseudilin | -7.67 ± 0.12 |
| 45 | Fucodiphloroethol G | -7.7 ± 0.17 |
| 46 | Octaphlorethol A | -9.43 ± 0.12 |
| 47 | Ellagic acid | -7.07 ± 0.06 |
| 48 | Diphlorethohydroxycarmalol | -8.03 ± 0.06 |
| 49 | Sargahydroquinoic acid | -6.07 ± 0.12 |
| 50 | Pheophorbide-A | -8.07 ± 0.12 |
| 51 | Benzene, 1,3-bis(1,1-dimethylethyl) | -6.43 ± 0.06 |
| 52 | 1-Hexadecene | -4.57 ± 0.06 |
| 53 | 8-Pentadecanone | -3.97 ± 0.12 |
| 54 | 8-Octadecanone | -4.57 ± 0.12 |
| 55 | Hexadecanoic acid | -4.8 ± 0 |
| 56 | Dibutyl phthalate | -5.27 ± 0.12 |
| 57 | Eicosyl acetate | -4.97 ± 0.12 |
| 58 | 10-Nonadecanone | -4.7 ± 0 |
| 59 | n-Nonadecanol-1 | -4.67 ± 0.06 |
| 60 | Methyl elaidate | -4.57 ± 0.12 |
| 61 | cis-11-Octadecenoic acid methyl ester | -5.53 ± 0.06 |
| 62 | Oxirane, hexadecyl | -4.23 ± 0.06 |
| 63 | Methyl stearate | -4.67 ± 0.12 |
| 64 | 14-Pentadecenoic acid | -5.07 ± 0.12 |
| 65 | Octadecanoic acid | -5.37 ± 0.12 |
| 66 | Tridecane, 3-methylene | -4.63 ± 0.06 |
| 67 | Docosanol | -5 ± 0 |

| | | |
|---|---|---|
| 68 | Octadecyl acetate | -4.9 ± 0 |
| 69 | Bis(2-ethylhexyl) adipate | -5.07 ± 0.12 |
| 70 | 1-Heptacosanol | -4.23 ± 0.06 |
| 71 | 1-Octacosanol | -5.47 ± 0.12 |
| 72 | Octatriacontyl trifluoroacetate | -4.07 ± 0.12 |
| 73 | 2-Hydroperoxypentane | -4.47 ± 0.12 |
| 74 | Nonyl trifluoroacetate | -4.87 ± 0.12 |
| 75 | 2,3-Heptanedione | -4.1 ± 0 |
| 76 | Dodecyl trifluoroacetate | -4.93 ± 0.06 |
| 77 | 2-Bromo-1-fluorododecane | -4.4 ± 0 |
| 78 | hexamethyl-3 trimethyl | -6.43 ± 0.06 |
| 79 | Dibutyl phthalate | -4.07 ± 0.06 |
| 80 | Octatriacontyl trifluoroacetate | -3.7 ± 0 |
| 81 | Paulomycin G | -6.97 ± 0.12 |
| 82 | Microindolinone A | -5.47 ± 0.12 |
| 83 | Sonalimycin | -7.27 ± 0.12 |
| 84 | Borrelidin | -7 ± 0.17 |
| 85 | Petrocidin A | -6.77 ± 0.06 |
| 86 | Rifamycin B | -7.33 ± 0.06 |
| 87 | Actinonin | -6.23 ± 0.06 |
| 88 | Xiamenmycin | -6.8 ± 0 |
| 89 | Manzamine A | -8.23 ± 0.06 |
| 90 | 2-Methyl butyl propyl pthalate | -4.83 ± 0.06 |
| 91 | Dinactin | -8.6 ± 0 |
| 92 | 4S-4,11-dihydroxy-10-methyl-dodec-2-en-1,4-olide | -6 ± 0 |
| 93 | Violapyrone B | -5.33 ± 0.06 |
| 94 | Isomethoxyneihumicin | -7.23 ± 0.06 |
| 95 | Quinomycin G | -7.63 ± 0.06 |
| 96 | Fredericamycin A | -8.43 ± 0.06 |
| 97 | Marangucycline A | -6.8 ± 0 |
| 98 | Isopimara-2-one-3-ol-8,15-diene | -8.53 ± 0.06 |
| 99 | Isoikarungamycin | -5.97 ± 0.12 |
| 100 | Bohemamine | -8.7 ± 0 |
| 101 | Thiasporine A | -5.97 ± 0.12 |
| 102 | 3-(4-Hydroxyphenyl)-N-methylpropanamide | -5.97 ± 0.06 |

| | | |
|---|---|---|
| 103 | Lagumycin B | -5.87 ± 0.06 |
| 104 | Sioxanthin | -9.1 ± 0 |
| 105 | Andrimid | -7.43 ± 0.06 |
| 106 | Moiramide | -7.23 ± 0.06 |
| 107 | Althiomycin | -4.7 ± 0.17 |
| 108 | Undecylprodigiosin | -7.23 ± 0.06 |
| 109 | Cycloprodigiosin | -5.83 ± 0.06 |
| 110 | Prodigiosin | -7.43 ± 0.06 |
| 111 | Astaxanthin | -6.67 ± 0.12 |
| 112 | Violacein | -6.77 ± 0.12 |
| 113 | Pyocyanin | -8.23 ± 0.06 |
| 114 | Phenazine-1-carboxylic acid | -6.97 ± 0.12 |
| 115 | Fridamycin D | -6.93 ± 0.23 |
| 116 | Himalomycin A | -7 ± 0.17 |
| 117 | Himalomycin B | -7.87 ± 0.06 |
| 118 | Chinikomycin B | -7.57 ± 0.06 |
| 119 | Manumycin A | -7.03 ± 0.12 |
| 120 | Loloatin B | -8.03 ± 0.06 |
| 121 | Bacillamide | -7.6 ± 0.17 |
| 122 | Macrolactin S | -6.6 ± 0 |
| 123 | Macrolactin V | -6.87 ± 0.06 |
| 124 | Fucoidan | -7.13 ± 0.12 |
| 125 | Sargachromanol G | -5.63 ± 0.06 |
| 126 | Floridoside | -6.9 ± 0.35 |
| 127 | Symbiomine | -7.1 ± 0.17 |
| 128 | Phorbaketal A | -7.1 ± 0 |
| 129 | Norzoanthamine | -7.6 ± 0 |
| 130 | lipoxazolidinone A | -8.2 ± 0 |
| 131 | lipoxazolidinone B | -5.73 ± 0.06 |
| 132 | lipoxazolidinone C | -5.73 ± 0.12 |
| 133 | ayamycin | -5.4 ± 0.17 |
| 134 | asphodelin | -5.53 ± 0.92 |
| 135 | Pentabromopseudilin | -5.43 ± 0.06 |
| 136 | progiodosin | -7.3 ± 0 |
| 137 | Tropodithietic acid | -6.53 ± 0.46 |

| | | |
|---|---|---|
| 138 | Nigribactin | -5.47 ± 0.06 |
| 139 | Abyssomycin | -6.77 ± 0.12 |
| 140 | Abyssomycin C | -8.43 ± 0.06 |
| 141 | Albidopyrone | -7.6 ± 0 |
| 142 | Bonactin | -7.23 ± 0.06 |
| 143 | Diazepinomicin | -8.37 ± 0.12 |
| 144 | Enterocin | -7.47 ± 0.12 |
| 145 | Frigoyclinone | -6.17 ± 0.12 |
| 146 | Gutingimycin | -6.37 ± 0.12 |
| 147 | Salinosporamide A | -7.27 ± 0.12 |
| 148 | Thiocoraline | -9.2 ± 0 |
| 149 | Thio peroxidase-1161 | -6.23 ± 0.06 |
| 150 | Aerothionin | -7.67 ± 0.12 |
| 151 | 4,5-dibromopyrrole-2-carboxylic acid | -4.73 ± 0.06 |
| 152 | Dibromophakellin (Alkaloids) | -6.3 ± 0 |
| 153 | Halistanol (Sterol) | -6.97 ± 0.12 |
| 154 | Plakinamine A | -6.8 ± 0 |
| 155 | Plakinamine B | -7.47 ± 0.06 |
| 156 | Furanoid | -5 ± 0 |
| 157 | Aeroplysinin | -4.83 ± 0.06 |
| 158 | Manoalide | -7.17 ± 0.06 |
| 159 | 6-hydroxymanzamine E | -9.4 ± 0 |
| 160 | Cribrostatin 3 | -6.5 ± 0 |
| 161 | Cribrostatin 6 | -6.67 ± 0.12 |
| 162 | Isojaspic acid | -7.67 ± 0.12 |
| 163 | Isoaaptamine | -6.17 ± 0.12 |
| 164 | (–)-Microcionin-1 | -8.37 ± 0.12 |
| 165 | Acanthosterol I | -6.9 ± 0 |
| 166 | Acanthosterol J | -7.13 ± 0.06 |
| 167 | Oceanapiside | -4.77 ± 0.12 |
| 168 | Spongistatin | -7.37 ± 0.12 |
| 169 | Leucascandrolide A | -5.53 ± 0.06 |
| 170 | Heteronemin | -7.3 ± 0.17 |
| 171 | Isoaaptamine | -6.47 ± 0.12 |
| 172 | Debromohymenialdisine | -6.63 ± 0.06 |

| | | |
|---|---|---|
| 173 | Peloruside A | -5.9 ± 0 |
| 174 | Elenic acid | -6 ± 0 |
| 175 | Naamine D | -5.87 ± 0.12 |
| 176 | Agelasphin 11 | -4.37 ± 0.12 |
| 177 | Discorhabdin D | -6.83 ± 0.06 |
| 178 | Plakortide P | -5.7 ± 0 |
| 179 | 24-methoxypetrosaspongia C | -8.13 ± 0.06 |
| 180 | Laulimalide | -7.57 ± 0.06 |
| 181 | Hemiasterlin | -6.73 ± 0.06 |
| 182 | Dictyostatin | -6.73 ± 0.06 |
| 183 | Halichondrin B | -9.6 ± 0 |
| 184 | Arenastatin A | -7.37 ± 0.12 |
| 185 | Latrunculin A | -7.57 ± 0.06 |
| 186 | Neoamphimedine | -7.63 ± 0.06 |
| 187 | Agosterol A | -6.9 ± 0 |
| 188 | Salicylihalamide A | -8.23 ± 0.06 |
| 189 | Discorhabdin D | -7 ± 0 |
| 190 | Callystatin A | -7.13 ± 0.06 |
| 191 | Tedanolide | -7.43 ± 0.06 |
| 192 | Makaluvamines | -7.53 ± 0.06 |
| 193 | iotrochamides B | -7.67 ± 0.12 |
| 194 | kalihinol A | -6.13 ± 0.06 |
| 195 | 8-hydroxymanzamine A | -8.37 ± 0.12 |
| 196 | stelletin B | -7.73 ± 0.06 |
| 197 | stelliferin A | -6 ± 0 |
| 198 | Carteramine A | -8.17 ± 0.12 |
| 199 | Pyrazin-2(1H)-one | -4.53 ± 0.06 |
| 200 | Cacospongionolide B | -7.37 ± 0.12 |
| 201 | Petrosaspongiolide M | -8.13 ± 0.06 |
| 202 | Hyrtiosal | -7.13 ± 0.06 |
| Standard | Semagacestat | -6.6 ± 0.1 |

Protein-ligand interactions are reinforced by hydrogen bonding (27-28), while stability is facilitated by hydrophobic interactions such as π-alkyl and alkyl interactions. Hydrophobic residues within enzyme active site pockets enhance binding energy (29-31). Salt bridges form through electrostatic attraction between oppositely charged residues, contributing significantly to interaction specificity (32).

β-secretase, also known as BACE-1, is a membrane-bound aspartate protease. It has five key domains viz cytoplasmic domain, a transmembrane domain, pro-catalytic domain, catalytic domain, and a signal peptide. It has a large proteolytic pocket accommodating about 11 amino acids (26, 33). Within β-secretase, the amino acid residues Asp32 and Asp228 constitute the catalytic diad within the enzyme's active site, playing a vital role in APP cleavage (25, 34). The enzyme comprises the N-terminal side encompassing P4, P3, P2, and P1 residues and the C-terminal side containing P4', P3', P2', and P1' residues, situated on both sides of the cleavage site. The N-terminal site, crucial for activities, possesses the addition of residual due to the expansive catalytic pocket of the β-secretase enzyme (35).

From the findings, it was evident that Octaphlorethol A exhibited binding to β-secretase binding energy was approximately - 9.43 kcal/mol (Fig. 2 (a) & (b)), while the standard, Semagacestat, demonstrated as binding energy around - 6.6 kcal/mol (Fig. 3 (a) & (b)). Similarly, the findings in Table 2 interactions suggest that both ligands and standards were bound within the catalytic pocket of their enzyme. Octaphlorethol A engaged with β-secretase through hydrophobic interaction, hydrogen bond, and π-cation interaction, whereas Semagacestat primarily interacted via hydrophobic interaction and hydrogen bond (Table 2). Octaphlorethol A has been found to inhibit beta-secretase activity, potentially reducing the formation of amyloid-beta peptides and their subsequent aggregation into plaques. This suggests that Octaphlorethol A from *Ishige foliacea* may have therapeutic potential in treating or preventing AD. Octaphlorethol A is one type of phlorotannin isolated via brown algae, *Ishige foliacea*. Studies show that Octaphlorethol A exhibits antidiabetic effects by increasing glucose uptake via glucose transporter -4. It has also shown that they possess antioxidant activities (36-37). Octaphlorethol A inhibits melanin synthesis and tyrosinase activity, thereby exerting a whitening effect that can potentially be used in the cosmetic therapy industry (38-39). It has also been shown to promote hair growth (40). Studies have demonstrated that Octaphlorethol A lowered high blood pressure by inhibiting the Angiotensin I-convert enzyme and promoting nitric oxide formation (41).

Table 2: Molecular Docking Interaction Analysis: Comparison of Ligand-Target Protein Interactions with Standard Drugs

| Ligand | Hydrogen-bond | Hydrophobic- interactions | π-cation interactions |
|---|---|---|---|
| Octaphlorethol A | Asp3, Phe7, Arg194, Arg195, Asp223, Lys224, Asn233, Arg235, Ser325, Ser328, Thr329 | Thr72, Arg195, Trp197 | Arg194, Arg195, Arg235 |
| Semagacestat (Standard) | Asn233, Arg235, Ser325, Ser328 | Thr72, Glu265, Gln326 | - |

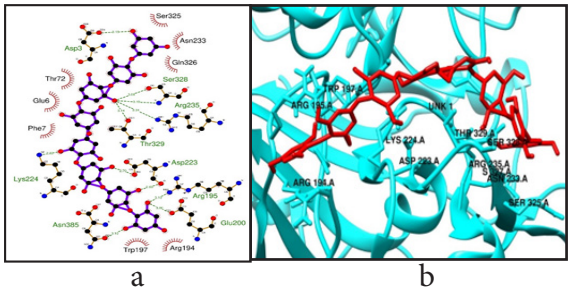

a b

Figure 2 (a) & (b): Interaction of the ligand Octaphlorethol-A with the enzyme β-secretase

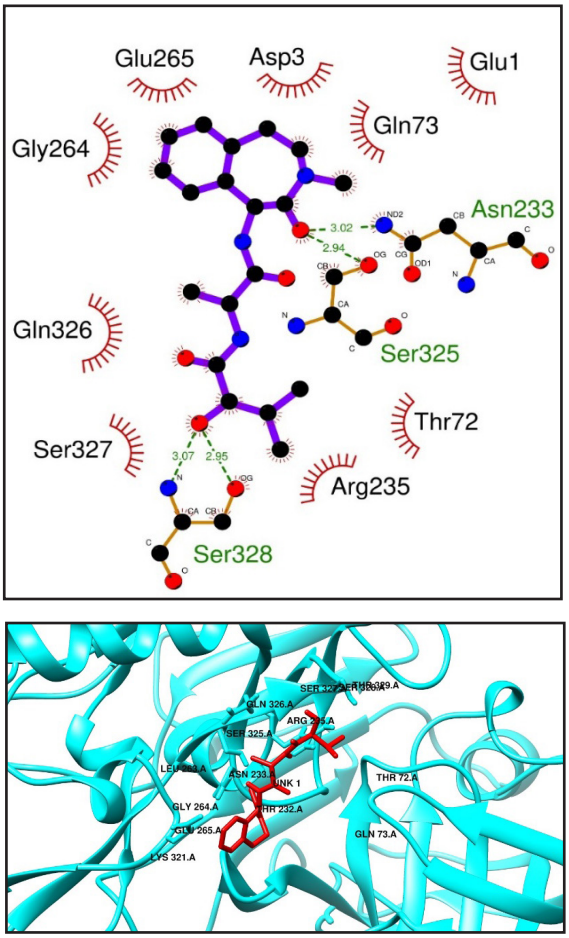


Figure 3 (a) & (b): Interaction of the Semagacestat with the enzyme β-secretase

### *MD simulations analysis*

The MD simulation studies give an in-depth understanding of protein-ligand interactions and their role in stabilizing ligand-bound states (42-43). This study analyzed the β secretase protein in complex with semagacestat (standard) and octaphlorethol (lead molecule) using 100 ns MD simulations. Trajectory files were analyzed using various GROMACS utilities to assess parameters including root mean square deviation (RMSD), root mean square fluctuation (RMSF), dynamics, radius of gyration, hydrogen bond, and solvent-accessible surface area.

### *Root mean square deviation (RMSD) analysis*

The RMSD plot scrutinized the backbone deviations in the protein-ligand interaction complexes during simulation (44). Fig. 4 reveals the RMSD values of the protein-semagacestat and protein-octaphlorethol complexes. It can be observed that both the complexes exhibited an increase in RMSD deviation with the simulation time range of 0–20 ns. Similarly, between 30 ns and 70 ns, minor variations in the RMSD pattern were seen. Towards the end of the 100 ns simulating, the standard (semagacestat) and the lead molecule (octaphlorethol) had RMSD values of 0.35 nm and 0.41 nm, respectively. Moreover, the standard and the lead molecule exhibited nearly identical RMSD fluctuation patterns. Hence, we suggest that the screened octaphlorethol compound may possess comparable inhibitory potential as semagacestat against β secretase protein.

### *Root mean square fluctuation (RMSF) analysis*

Root means square fluctuation (RMSF) determines protein residue flexibility within the protein-ligand complex. Fig. 5 illustrates the residue-wise fluctuations in the standard and hit complexes during 100 ns simulation. Peaks in the figure signify regions of heightened flexibility within the protein-ligand complex. Notably, residues Asp32, Gly34, Pro70, Thr72, Gln73, Arg128, Tyr198, Asp228, Gly230, and Thr232, which constitute the active site of β secretase, showed minimal fluctuation of ~0.03 nm upon

binding of semagacestat and octaphlorethol. Overall, the standard (semagacestat) and the lead (octaphlorethol) complex exhibited an average RMSF value around ~0.04 nm, indicating stable binding for the molecules within their active site of the β secretase protein.

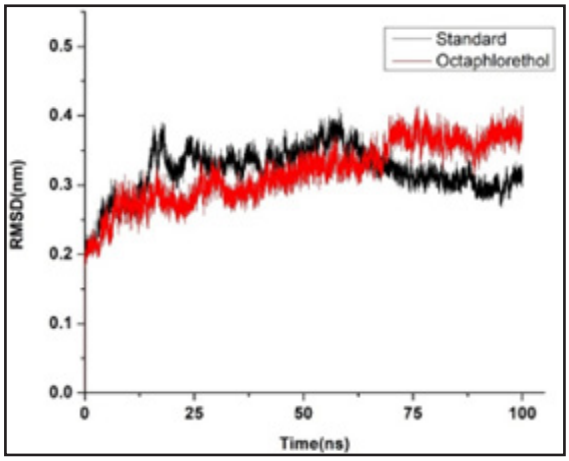


Figure 4: RMSD Plot of Protein-Ligand Complexes

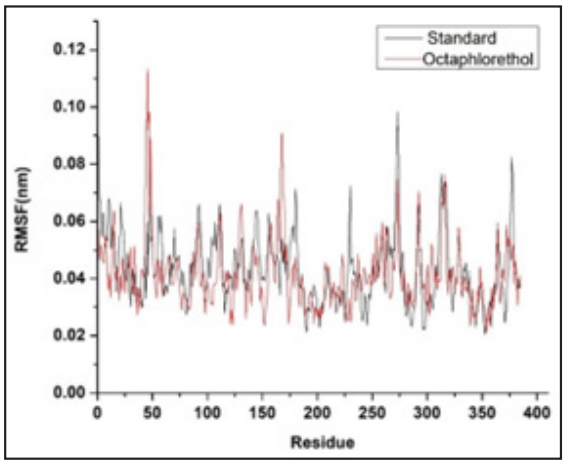


Figure 5: RMSF plot of protein-ligand complexes

**Analysis of hydrogen bonds**

Assessing hydrogen bond interactions is essential in determining the stabilization of a protein-ligand complex, which is crucial for protein foldage and molecule recognition (45). The existence of a hydrogen bond between β secretase - ligand complex was evaluated using the MD trajectory. According to the hydrogen bond plot in Fig. 6, the semagacestat (standard) complex generated an average of around four hydrogen bonds during their 100 ns simulation. In contrast, the octaphlorethol complexes generated 12 hydrogen bonds with the β secretase protein. Based on the outcome of the H-Bonding analysis, it can be inferred that octaphlorethol forms a more stable interaction with β secretase protein than semagacestat.

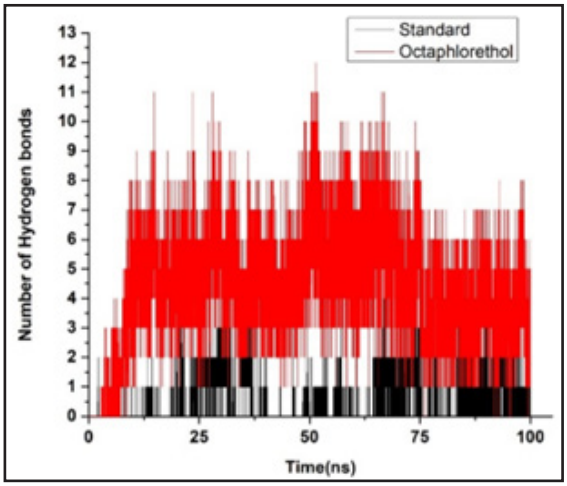


Figure 6: Hydrogen bond interactions of β secretase with ligand complexes

**Radius of gyration ($R_g$)**

The radius of gyration ($R_g$) sheds light on the stabilization and compaction of the protein-ligand complex. The $R_g$ is computed based on the weight of root mean square distances among the $C_\alpha$ atoms within the specified time frame (45). Simultaneously, from Fig. 7., it is observed that the average $R_g$ of β secretase-semagacestat and β secretase-octaphlorethol were found to be 2.11 nm and 2.17 nm. It is observed that though the binding of their hit compound imparts minimal modifications to the β secretase protein, it exhibits a nearly identical $R_g$ pattern as semagacestat.

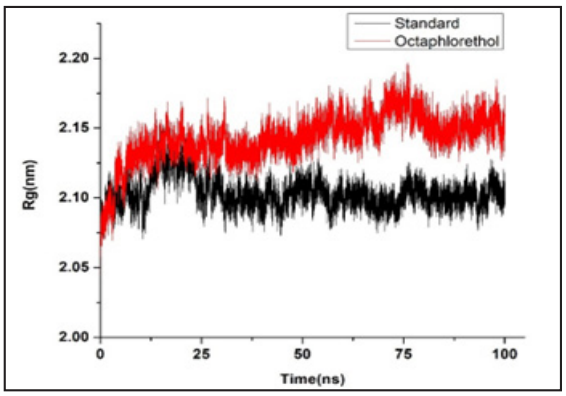


Figure 7: Radius of Gyration Plot of Protein-Ligand Complexes

### *Solvent accessible surface area (SASA)*

The solvent-accessible surface area (SASA) generally measures the protein's surface area and its interaction with the solvent through van der Waal's forces of attraction (46). Figure 5 shows the SASA plot for the complexes. The average SASA values for semagacestat and octaphlorethol were approximately 226.77 nm² and 228.58 nm², respectively. As evident from Figure 8, the SASA values for both semagacestat and octaphlorethol remained relatively stable throughout the 100 ns simulation. Therefore, the SASA plot indicates that the binding interactions of their hit molecule do not significantly affect the overall conformation of β-secretase.

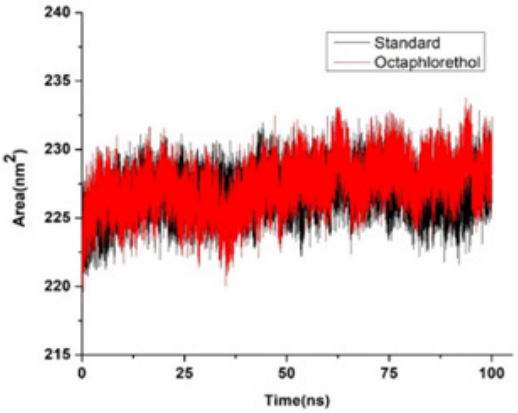


**Figure 8:** Solvent Accessible Surface Area Plot of Protein-Ligand Complexes

### ADMET analysis

Octaphlorethol A has a molecular weight of approx. 994.77 g/mol, with 14 rotatable bonds, 17 hydrogen bond donors, and 24 hydrogen bond acceptors. Its molar refractivity was about 246.44, and its topological polar surface area (TPSA) was around 408.52 Å². The Log Po/w (MLOGP) is approximately -0.59, indicating that the molecules were lipophilic and insoluble in water. The pharmacokinetic property reveals that Octaphlorethol A has low absorption in the gastrointestinal tract and does not permit blood-brain barriers. It acts as a substrate for P-glycoproteins and does not inhibit cytochrome P450 enzyme (1A2, 2C19, 2D6, 3A4), except for CYP2C9. Further, with a skin permeation Log Kp value of about -7.69 cm/s, it was a perfect skin permeable. The bio-availability score was 0.17. Toxicity predictions indicate that Octaphlorethol A is not hepatotoxic, carcinogenic, cytotoxic, mutagenic, or immunotoxic, with a predicted LD50 of 866 mg/kg.

### Conclusion

Secondary metabolites obtained from marine organisms exhibited a range of biological activity compared to their synthetic counterpart. In this study, 202 compounds derived using bacteria, actinomycetes, fungi, and algae were mined from the literature to assess their potential to inhibit β-secretase. The activities of these compounds were compared with the Semagacestat. Surprisingly, we could observe that the compound Octaphlorethol A demonstrates superior performance compared to the standard drug. Preliminary computational studies, including docking and molecular dynamic simulations, provided insights into the binding nature of these compounds to their target proteins. Additionally, the ADMET analysis indicated that these compounds possess the necessary pharmacokinetics and pharmacodynamics to be considered potential drug candidates. Further in-vitro and vivo studies are required to validate the potential of Octaphlorethol A against the β-secretase enzyme.

**Acknowledgment**

The authors would like to thank the National Institute of Technology, Andhra Pradesh and Vellore Institute of Technology, Vellore for providing the necessary facility to carry out this work.

**Funding**

This research did not receive any specific grant from funding agencies in the public, commercial, or not-for-profit sector.

**Disclosure Statement**

The authors declare that they have no conflicts of interest.

**Data availability Statement**

The data will be made available on request.

**References**

1. Morton, H., Kshirsagar, S., Orlov, E., Bunquin, L.E., Sawant, N., Boleng, L., George, M., Basu, T., Ramasubramanian, B., Pradeepkiran, J.A. and Kumar, S., 2021. Defective mitophagy and synaptic degeneration in Alzheimer's disease: Focus on aging, mitochondria and synapse. *Free Radical Biology and Medicine*, *172*, pp.652-667.
2. Nichols, E. and Vos, T., 2021. The estimation of the global prevalence of dementia from 1990-2019 and forecasted prevalence through 2050: an analysis for the Global Burden of Disease (GBD) study 2019. *Alzheimer's & Dementia*, *17*, p.e051496.
3. Atri, A., 2019. The Alzheimer's disease clinical spectrum: diagnosis and management. *Medical Clinics*, *103*(2), pp.263-293.
4. Abraham, J.T., Maharifa, H.N.S. and Hemalatha, S., 2022. In silico molecular docking approach against enzymes causing Alzheimer's disease using Borassus flabellifer Linn. *Applied Biochemistry and Biotechnology*, 194, pp.1804–1813.
5. Bojić, T., Sencanski, M., Perovic, V., Milicevic, J. and Glisic, S., 2022. In silico screening of natural compounds for candidates 5HT6 receptor antagonists against Alzheimer's disease. *Molecules*, *27*(9), pp.2626.
6. Decourt, B., D'Souza, G.X., Shi, J., Ritter, A., Suazo, J. and Sabbagh, M.N., 2022. The cause of Alzheimer's disease: the theory of multipathology convergence to chronic neuronal stress. *Aging and disease*, *13*(1), pp.37.
7. Pająk, B., Kania, E. and Orzechowski, A., 2016. Killing me softly: connotations to unfolded protein response and oxidative stress in Alzheimer's disease. *Oxidative medicine and cellular longevity*, *2016*(1), pp.1805304.
8. Kametani, F. and Hasegawa, M., 2018. Reconsideration of amyloid hypothesis and tau hypothesis in Alzheimer's disease. *Frontiers in neuroscience*, *12*, pp.328460.
9. Frozza, R.L., Lourenco, M.V. and De Felice, F.G., 2018. Challenges for Alzheimer's disease therapy: insights from novel mechanisms beyond memory defects. *Frontiers in neuroscience*, *12*, pp. 334515.
10. Chakraborty, B., Kumar, R.S., Almansour, A.I., Gunasekaran, P. and Nayaka, S., 2022. Bioprospection and secondary metabolites profiling of marine Streptomyces levis strain KS46. *Saudi Journal of Biological Sciences*, *29*(2), pp.667-679.
11. Kizhakedathil, M.P. and Chandrasekaran, S.D., 2018. Screening for extracellular enzymes from actinomycetes isolated from agricultural soils of Kolathur, Tamil Nadu, India. *Current Bioactive Compounds*, *14*(4), pp.387-396.
12. Sarkar, G. and Suthindhiran, K., 2022. Diversity and biotechnological potential of

marine actinomycetes from India. *Indian Journal of Microbiology*, *62*(4), pp.475-493.

13. Genovese, M., Nesi, I., Caselli, A. and Paoli, P., 2021. Natural α-glucosidase and protein tyrosine phosphatase 1B inhibitors: A source of scaffold molecules for synthesis of new multitarget antidiabetic drugs. Molecules, 26(16), p.4818.
14. Mahapatra, G.P., Raman, S., Nayak, S., Gouda, S., Das, G. and Patra, J.K., 2020. Metagenomics approaches in discovery and development of new bioactive compounds from marine actinomycetes. Current Microbiology, 77, pp.645-656.
15. Rengasamy, K.R., Mahomoodally, M.F., Aumeeruddy, M.Z., Zengin, G., Xiao, J. and Kim, D.H., 2020. Bioactive compounds in seaweeds: An overview of their biological properties and safety. Food and Chemical Toxicology, 135, pp.111013.
16. Pettersen, E.F., Goddard, T.D., Huang, C.C., Couch, G.S., Greenblatt, D.M., Meng, E.C. and Ferrin, T.E., 2004. UCSF Chimera—a visualization system for exploratory research and analysis. *Journal of computational chemistry*, *25*(13), pp.1605-1612.
17. Hong, L., Turner, R.T., Koelsch, G., Shin, D., Ghosh, A.K. and Tang, J., 2002. Crystal structure of memapsin 2 (β-secretase) in complex with an inhibitor OM00-3. *Biochemistry*, *41*(36), pp.10963-10967.
18. Yuan, S., Chan, H.S. and Hu, Z., 2017. Using PyMOL as a platform for computational drug design. Wiley Interdisciplinary Reviews: Computational Molecular Science, 7(2), p.e1298.
19. Eberhardt, J., Santos-Martins, D., Tillack, A.F. and Forli, S., 2021. AutoDock Vina 1.2. 0: New docking methods, expanded force field, and python bindings. Journal of chemical information and modeling, 61(8), pp.3891-3898.
20. Trott, O. and Olson, A.J., 2010. AutoDock Vina: improving the speed and accuracy of docking with a new scoring function, efficient optimization, and multithreading. Journal of computational chemistry, 31(2), pp.455-461.
21. Salentin, S., Schreiber, S., Haupt, V.J., Adasme, M.F. and Schroeder, M., 2015. PLIP: fully automated protein–ligand interaction profiler. Nucleic acids research, 43(W1), pp.W443-W447.
22. Laskowski, R.A. and Swindells, M.B., 2011. LigPlot+: multiple ligand–protein interaction diagrams for drug discovery. Journal of Chemical Information and Modeling, 51(10), pp. 2778–2786.
23. Daina, A., Michielin, O. and Zoete, V., 2017. SwissADME: a free web tool to evaluate pharmacokinetics, drug-likeness and medicinal chemistry friendliness of small molecules. Scientific reports, 7(1), p.42717.
24. Banerjee, P., Eckert, A.O., Schrey, A.K. and Preissner, R., 2018. ProTox-II: a webserver for the prediction of toxicity of chemicals. Nucleic acids research, 46(W1), pp.W257-W263.
25. Ullah, M.A., Johora, F.T., Sarkar, B., Araf, Y., Ahmed, N., Nahar, A.N. and Akter, T., 2021. Computer-assisted evaluation of plant-derived β-secretase inhibitors in Alzheimer's disease. Egyptian Journal of Medical Human Genetics, 22, pp.1-15.
26. Frimayanti, N., Aryani, F., Rishanti, N. and Yaeghoobi, M., 2021, October. In silico analysis towards exploring potential β secretase 1 (BACE1) inhibitors; the cause of Alzhemier disease. In Journal of Physics: Conference Series, 2049 (1), p. 012011.
27. Loganathan, Y., Jain, M., Thiyagarajan, S., Shanmuganathan, S., Mariappan, S.K.,

Kizhakedathil, M.P.J. and Saravanakumar, T., 2021. An Insilico evaluation of phytocompounds from Albizia amara and Phyla nodiflora as cyclooxygenase-2 enzyme inhibitors. DARU Journal of Pharmaceutical Sciences, 29(2), pp.311-320.

28. Kizhakedathil, M.P.J., Madasu, P.K., Chandran, T. and Vijaykumar, S.D., 2023. In-silico structural studies on anti-inflammatory activity of phytocompounds from the genus Andrographis. Journal of Biomolecular Structure and Dynamics, pp.1-13.

29. Tabassum, S., Ahmad, S., Rehman Khan, K.U., Tabassum, F., Khursheed, A., Zaman, Q.U., Bukhari, N.A., Alfagham, A., Hatamleh, A.A. and Chen, Y., 2022. Phytochemical profiling, antioxidant, anti-inflammatory, thrombolytic, hemolytic activity in vitro and in silico potential of Portulacaria afra. Molecules, 27(8), pp.2377.

30. Prabhavathi, H., Dasegowda, K.R., Renukananda, K.H., Lingaraju, K. and Naika, H.R., 2021. Exploration and evaluation of bioactive phytocompounds against BRCA proteins by in silico approach. Journal of Biomolecular Structure and Dynamics, 39(15), pp.5471-5485.

31. Daze, K., Hof, F., 2016. Molecular interaction and recognition, In: Wang, Z., (Ed), Encyclopedia of physical organic chemistry, John Wiley & Sons. Inc., New Jersey, pp. 1-51.

32. Bosshard, H.R., Marti, D.N. and Jelesarov, I., 2004. Protein stabilization by salt bridges: concepts, experimental approaches and clarification of some misunderstandings. Journal of Molecular Recognition, 17(1), pp.1-16.

33. Galeana-Ascencio, R.A., Mendieta, L., Limon, D.I., Gnecco, D., Terán, J.L., Orea, M.L. and Carrasco-Carballo, A., 2023. β-Secretase-1: In Silico Drug Reposition for Alzheimer's Disease. International Journal of Molecular Sciences, 24(9), pp.8164.

34. Huang, D., Lüthi, U., Kolb, P., Cecchini, M., Barberis, A. and Caflisch, A., 2006. In silico discovery of β-secretase inhibitors. Journal of the American Chemical Society, 128(16), pp.5436-5443.

35. Venugopal, C., Demos, C.M., Jagannatha Rao, K.S., Pappolla, M.A. and Sambamurti, K., 2008. Beta-secretase: structure, function, and evolution. CNS & Neurological Disorders-Drug Targets (Formerly Current Drug Targets-CNS & Neurological Disorders), 7(3), pp.278-294.

36. Lee, S.H., Kang, S.M., Ko, S.C., Lee, D.H. and Jeon, Y.J., 2012. Octaphlorethol A, a novel phenolic compound isolated from a brown alga, Ishige foliacea, increases glucose transporter 4-mediated glucose uptake in skeletal muscle cells. Biochemical and biophysical research communications, 420(3), pp.576-581.

37. Lee, S.H., Kang, N., Kim, E.A., Heo, S.J., Moon, S.H., Jeon, B.T. and Jeon, Y.J., 2014. Antidiabetogenic and antioxidative effects of octaphlorethol a isolated from the brown algae Ishige foliacea in streptozotocin-induced diabetic mice. Food science and biotechnology, 23, pp.1261-1266.

38. Kim, K.N., Yang, H.M., Kang, S.M., Kim, D., Ahn, G. and Jeon, Y.J., 2013. Octaphlorethol A isolated from Ishige foliacea inhibits α-MSH-stimulated induced melanogenesis via ERK pathway in B16F10 melanoma cells. Food and chemical toxicology, 59, pp.521-526.

39. Kim, K.N., Yang, H.M., Kang, S.M., Ahn, G., Roh, S.W., Lee, W., Kim, D. and Jeon, Y.J., 2015. Whitening effect of octaphlorethol A isolated from Ishige foliacea in an in vivo zebrafish model. Journal of Microbiology and Biotechnology, 25(4), pp.448-451.

40. Kang, J.I., Kim, E.J., Kim, M.K., Jeon, Y.J., Kang, S.M., Koh, Y.S., Yoo, E.S. and

Kang, H.K., 2013. The promoting effect of Ishige sinicola on hair growth. Marine drugs, 11(6), pp.1783-1799.

41. Ko, S.C., Jung, W.K., Kang, S.M., Lee, S.H., Kang, M.C., Heo, S.J., Kang, K.H., Kim, Y.T., Park, S.J., Jeong, Y. and Kim, M., 2015. Angiotensin I-converting enzyme (ACE) inhibition and nitric oxide (NO)-mediated antihypertensive effect of octaphlorethol A isolated from Ishige sinicola: In vitro molecular mechanism and in vivo SHR model. Journal of functional foods, 18, pp.289-299.

42. Shahroz, M.M., Sharma, H.K., Altamimi, A.S., Alamri, M.A., Ali, A., Ali, A., Alqahtani, S., Altharawi, A., Alabbas, A.B., Alossaimi, M.A. and Riadi, Y., 2022. Novel and potential small molecule scaffolds as DYRK1A inhibitors by integrated molecular docking-based virtual screening and dynamics simulation study. Molecules, 27(4), p.1159.

43. Ramesh, P., Shin, W.H. and Veerappapillai, S., 2021. Discovery of a potent candidate for ret-specific non-small-cell lung cancer—a combined in silico and in vitro strategy. Pharmaceutics, 13(11), p.1775.

44. Singh, A., Singh, A., Grover, S., Pandey, B., Kumari, A. and Grover, A., 2018. Wild-type catalase peroxidase vs G279D mutant type: Molecular basis of Isoniazid drug resistance in Mycobacterium tuberculosis. Gene, 641, pp.226-234.

45. Murali, P. and Karuppasamy, R., 2023. Imidazole and biphenyl derivatives as anti-cancer agents for glioma therapeutics: Computational drug repurposing strategy. Anti-Cancer Agents in Medicinal Chemistry (Formerly Current Medicinal Chemistry-Anti-Cancer Agents), 23(9), pp.1085-1101.

46. Saini, G., Dalal, V., Savita, B.K., Sharma, N., Kumar, P. and Sharma, A.K., 2019. Molecular docking and dynamic approach to virtual screen inhibitors against Esbp of Candidatus Liberibacter asiaticus. *Journal of Molecular Graphics and Modelling*, *92*,pp.329-340.